

Supporting Information for

Limited earthquake interaction during a geothermal hydraulic stimulation in Helsinki, Finland

Grzegorz Kwiatek¹, Patricia Martínez-Garzón¹, Jörn Davidsen^{2,3}, Peter Malin⁴, Aino Karjalainen⁵, Marco Bohnhoff^{1,6}, and Georg Dresen^{1,7}

1. Section 4.2 Geomechanics and Scientific Drilling, Helmholtz Centre Potsdam, GFZ German Research Centre for Geosciences, Potsdam, Germany.
2. Complexity Science Group, Department of Physics and Astronomy, University of Calgary, Canada.
3. Hotchkiss Brain Institute, University of Calgary, Canada.
4. ASIR Advanced Seismic Instrumentation and Research, Dallas, TX, USA
5. St1 Oy, Helsinki, Finland
6. Department of Earth Sciences, Institute of Geological Sciences, Free University Berlin, Berlin, Germany
7. Institute of Earth and Environmental Science, University of Potsdam, Potsdam, Germany

Contents of this file

Figures S1 to S3
Data Set S1

Introduction

This supplementary information contains additional figures presenting biases to different statistical properties introduced by inappropriate assumptions to magnitude of completeness in the analyzed catalog.

Figure S1. Differences in the probability to observe a magnitude difference $M_{i+1} - M_i < \Delta m$ between selected subset of the catalog containing N earthquakes (black dots) and its randomized versions, which do not exhibit magnitude correlations (eq. 3, dark and light magenta areas correspond to 95% and 68% confidence intervals). Magnitude correlations correspond to significant deviations from zero. Events above $M_C = -1.44$ were used, thus including the periods of catalog incompleteness due to day-night anthropogenic noise cycles and pumping noise oscillations leading to spurious magnitude correlations in case of phases P1 and P2-P4. (a): Phase P1; (b): Phases P2-P4; (c): Phase P3; (d): Post-stimulation seismicity (cf. Fig. 2 for time intervals)

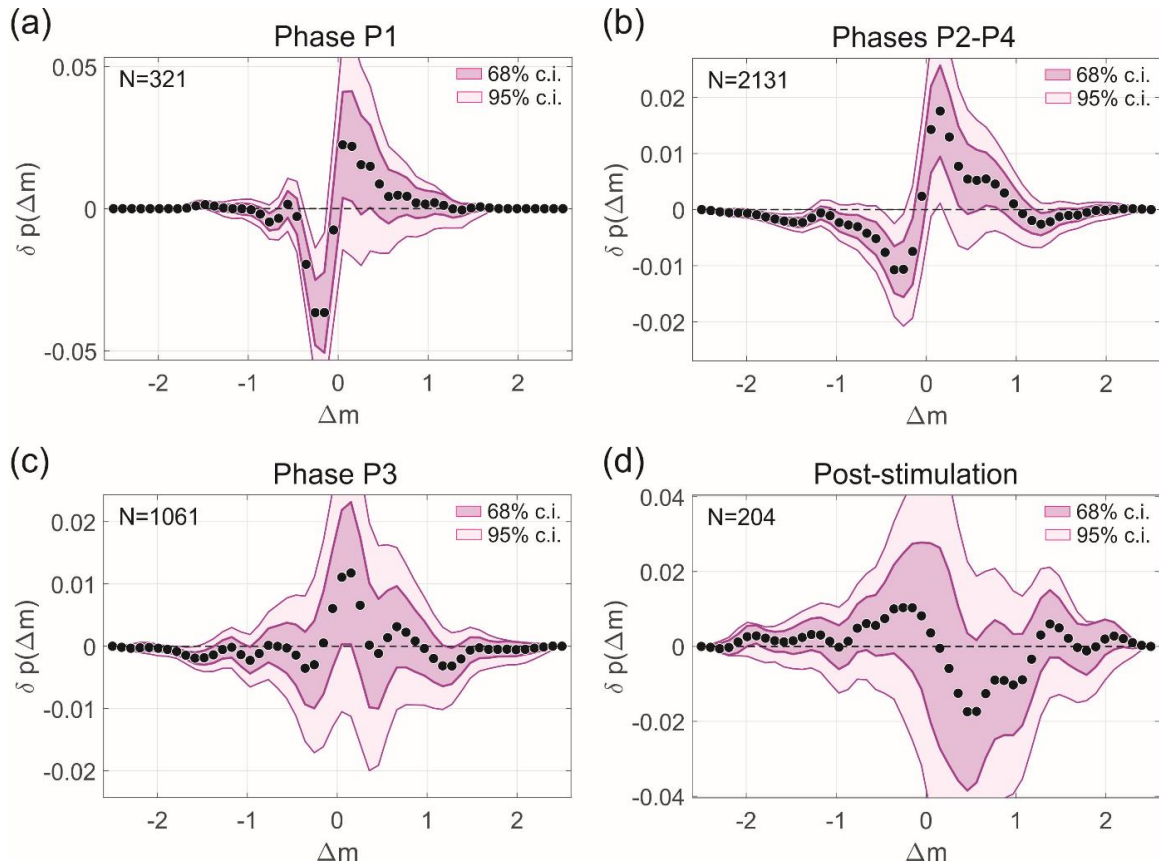


Figure S2. Probability density function of interevent time ratios, $p(R)$, for seismicity from different phases of 2020 stimulation and above the conservative magnitude of completeness, $M_C^* = -1.25$ (cf. Fig. 8a-d). Input data is conditioned on the difference in magnitudes of adjacent events (larger events preceding the small ones promotes aftershock sequences). (a): Phase P1; (b) Phase P2-P4; (c): Phase P3; (d) Post-stimulation. Solid and dashed red lines correspond to 68% and 95% confidence intervals of $p(R)$ expected from events randomly distributed in time, assuming same number of events as in the particular catalog subset.

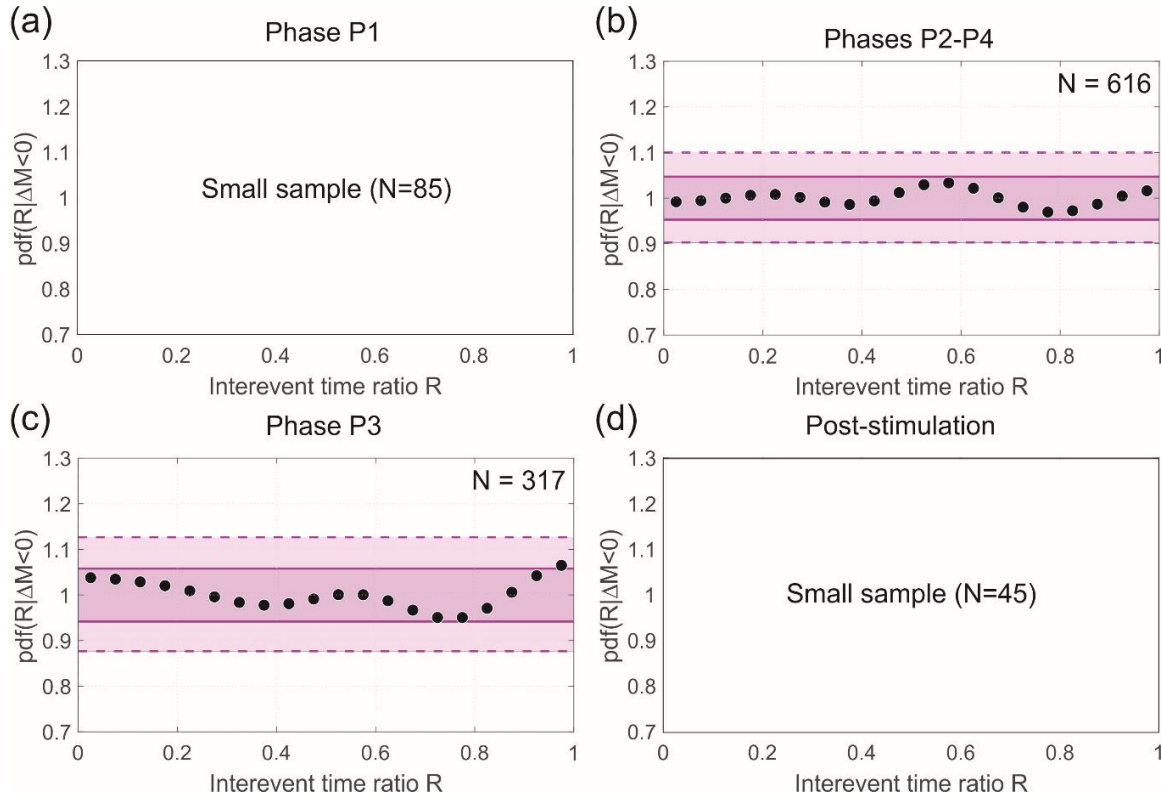
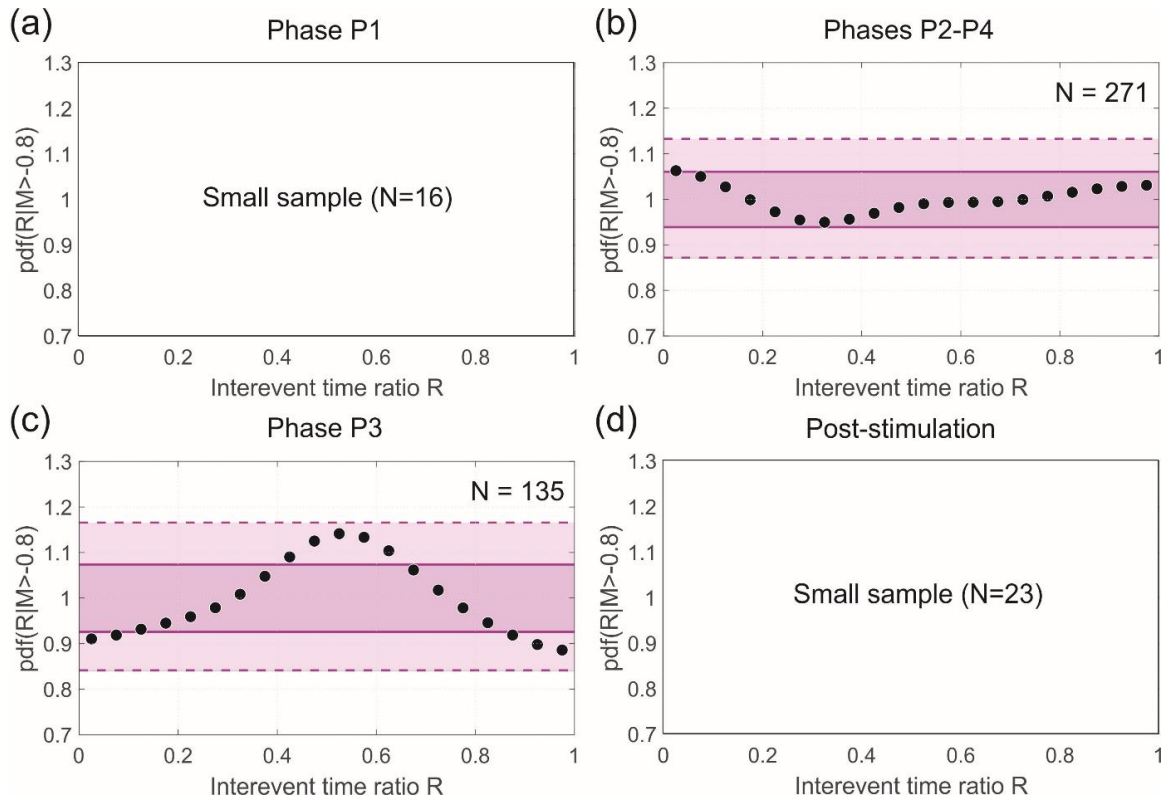


Figure S3. Probability density function of interevent time ratios, $p(R)$, for seismicity from different phases of 2020 stimulation and above the conservative magnitude of completeness, $M_C^* = -1.25$ (cf. Fig. 8a-d). Input data is conditioned on the magnitude of events (larger events are expected to trigger more frequently). (a): Phase P1; (b) Phase P2-P4; (c): Phase P3; (d) Post-stimulation. Solid and dashed red lines correspond to 68% and 95% confidence intervals of $p(R)$ expected from events randomly distributed in time, assuming same number of events as in the particular catalog subset.



Data Set S1. Catalog of detections, located and relocated events and focal mechanisms is available as separate data publication:

Kwiatek, Grzegorz; Martínez-Garzón, Patricia; Karjalainen, Aino (2026): Earthquake catalog of induced seismicity associated with 2020 hydraulic stimulation campaign at OTN-2 well in Helsinki, Finland. GFZ Data Services, DOI: 10.5880/GFZ.4.2.2022.001 (THIS IS A TEMPORARY LINK TO DATA PUBLICATION: <https://dataservices.gfz-potsdam.de/panmetaworks/review/a2cbf70b76bb7986442617ccf186d6c05d1c78b8da75888748b4401e6dceb24c/>).